



ELSEVIER

Available online at www.sciencedirect.com

SCIENCE @ DIRECT®

Neurocomputing ■ (■■■■) ■■■-■■■

NEUROCOMPUTING

www.elsevier.com/locate/neucom

Letters

A new methodology for in situ calibration of a neural network-based software sensor for S -parameter prediction in six-port reflectometers

J.L. Pedreño-Molina^a, M. Pinzolas^{b,*}, J. Monzó-Cabrera^a^aDepartment of Information Technologies and Communications, Technical University of Cartagena, Campus Muralla del Mar s/n, E-30.202, Cartagena, Murcia, Spain^bDepartment of System Engineering and Automation, Technical University of Cartagena, Campus Muralla del Mar s/n, E-30.202, Cartagena, Murcia, Spain

Received 16 September 2005; received in revised form 23 January 2006; accepted 24 January 2006

Communicated by R.W. Newcomb

Abstract

In this work, a neural network-based software sensor is proposed for determining the reflection coefficient from measurements obtained by a six-port reflectometer. The proposed software sensor is able to cope with the nonlinearities and noise inherent to the measurement electronics, without needing additional calibration. To extract data for the calibration, a new method that allows in situ calibration is applied. Experimental evidence of the feasibility of the proposed method is given using a simulation testbench.

© 2006 Published by Elsevier B.V.

Keywords: Six-port reflectometer; S -parameter prediction; Six-port calibration; Neural networks; Microwave cavity measurements

1. Introduction

Techniques for scattering parameter measurements in microwave structures are still being developed for applications such as drying, heating, modeling or circuit design. Traditional methods for these techniques are based in *slotted lines* or *impedance bridges* [16]. Other methods consist on circuit designs based on directional couplers to separate the incident and reflected wave power (*reflectometers*) and to determine the amplitude (escalar) and phase (vectorial) of the reflection coefficient. However, the most extended methods for impedance measurement are the so called *six-port reflectometer* [2] and the *network analyzers*. On the one hand, the six-port, designed by Engen in 1977, is an inexpensive solution that avoids the use of network analyzers; on the other hand, it employs simple power detectors (like diodes or thermistors) in opposition to the mixers of the analyzers. It consists in a simple circuit with six ports connected to the source (a *magnetron* in this case), the unknown load and four power detectors. From the outputs of the detectors, a numerical

relationship can be obtained to determine the reflection coefficient in the load. This numerical expression combines the value of several parameters, very sensitive to measurement noises, in order to determine the desired impedance value given by $S_{11} = b_2/a_2$, as Fig. 1 shows.

Besides the noise, the effect of nonlinearity in the detectors for the considered frequencies implies the calibration of both six-port and detectors to guarantee the accuracy of the measurements. Several techniques have been published for calibration of six-port parameters by considering effects such as measurement dynamic range and diode nonlinearity [8,12]. Six-port parameter calibration is based on finding the numerical solution for the equation system given by (1), being M_i and N_i complex constants, which must be obtained from the measured values b_i and a_i :

$$\begin{aligned} b_3 &= M_3 a_2 + N_3 b_2, \\ b_4 &= M_4 a_2 + N_4 b_2, \\ b_5 &= M_5 a_2 + N_5 b_2, \\ b_6 &= M_6 a_2 + N_6 b_2. \end{aligned} \quad (1)$$

The moduli of the $\{b_3, b_4, b_5, b_6\}$ coefficients can be estimated from the $\{v_3, v_4, v_5, v_6\}$ values (usually voltages)

*Corresponding author. Tel.: +34 968 325477; fax: +34 968 325455.

E-mail address: miguel.pinzolas@upct.es (M. Pinzolas).

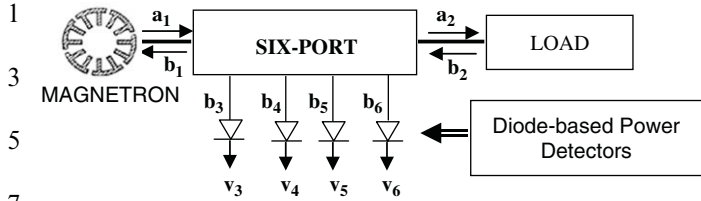


Fig. 1. Six-port scheme. Incident and emergent scattering variables at the i th-port are represented by a_i and b_i .

quality of connectors and transmission lines or instability and bad resolution in the diodes produce increments in the final calibration error. In order to improve the accuracy of the calibration, some techniques are being proposed by incorporating the diode effects in the calibration procedure. Thus, linear approximation of the diode response around the work frequency is developed in Refs. [8,18,19] or in Ref. [6], where a temperature dependent corrector factor is added for minimizing the error for a wide bandwidth. Moreau et al. [12] employed a sliding termination for the simultaneous calibration of both the diode and the six-port, doubling the number of parameters to be estimated. Other alternatives [7] have been proposed by using thermistors as power detectors instead of semiconductor diodes, increasing the measurement accuracy. More complex diode characteristics are considered in Ref. [1], where a precise variable attenuator at the input of the six-port is used for the calibration. Finally a method based on artificial neural networks is described in Ref. [10] for both the six-port and diode calibration.

Until now, all the described methods rely on the use of specially designed devices, such as variable loads and attenuators/phase-shifters. Recently, some empirical results have shown that the reflection coefficient varies as the distance of the load from the magnetron is varied [13,15]. This variation is mainly due to interference among the source waves coming from the magnetron, and the ones reflected from the load. When represented against the distance of the load from the magnetron, the reflection coefficient shows a clear periodic pattern, as can be seen in Fig. 2. These variations appear wherever the dielectric constant of the load is different from the one of the material inside the cavity (usually air), so that almost any material can be used.

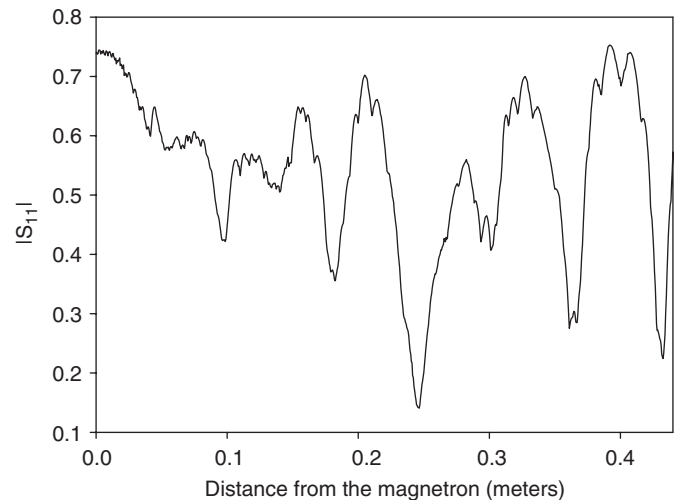


Fig. 2. Variation of the reflection coefficient $|S_{11}|$ as the sample being irradiated changes its distance from the magnetron. Data are extracted from an experiment carried out with the experimental set-up described in Section 2, using a sample with dielectric constant $\epsilon' = 20$ and loss factor $\epsilon'' = 5j$.

given by the corresponding detectors (usually diodes, see Fig. 1). The relationship $S_{11} = b_2/a_2$ is obtained by means of measurements of load impedance.

The most extended technique for determining the M_i and N_i parameters is based on ending the six-port with at least four standard loads [16], sliding terminations [3,12] or TRL (thru-reflect-line) method [9] whose parameters are obtained from the type of material and physical dimension of the employed transmission lines. In Ref. [19] five loads with the same module are used for the calibration, in order to eliminate ill-conditioned configurations. In this way, the numerical solution can be graphically represented in the complex plane of impedances, by means of three circles, whose intersection gives the desired solution for S_{11} . Other authors as Engen [3] or Wiedmann et al. [19] employ the six-port to four-port technique by reducing the number of parameters in Eq. (1) to three, by exploiting the circular symmetries with respect to the complex axes.

In fact and due to measurement errors and noises, the intersection is a small area and not only one point. In this way, efforts have been made to numerically find the solution in the presence of noise and software for online calibration [17]. One example can be found in Ref. [4] where a procedure based on least-squared methods is developed, when Gaussian distributions for the mean power errors are considered. In Ref. [20], a new calibration method based on the closeness of the Fourier coefficients of the six-port parameters and the port power ratios of each standard load is presented.

Most advanced techniques, including online computation, have been designed to improve the last calibration techniques. Thus, in Ref. [14] Rangel et al. present a method based on numerical relationships from the measurement of signals with different frequencies, which are inputs to the reflectometer and one application software. In order to avoid the complex manufacturing of sliding loads, Yakabe et al. propose in Ref. [21] a calibration method based on active load synthesis by computer, by autonomously adjusting one phase shifter and one attenuator.

The methods above have been designed without taking into account the nonlinearity effect of the diodes in the six-port. This nonlinearity exacerbates when high input level is considered. A square-law characteristic is normally considered for the relationship between the detected power and the output voltage in each diode. Indeed, effects such as

In this paper, this fact is exploited to propose a new calibration method for the six-port. As in Ref. [10], a neural network architecture is used to cope with nonlinearities appearing in the diodes, and to find the relation between the measured quantities and the reflection coefficient. Because the six-port reflectometer is only designed to measure $|S_{11}|$ as a ratio of the real values for the incident and reflected power, the phase of S_{11} has not been considered. The estimation for the phase needs other measurement schemes such as vectorial network analyzers.

As a difference, both training and validation data are extracted without using especial devices, simply irradiating a sample of any material at different distances from the magnetron.

The viability of the proposed calibration method is studied in simulation, as a prior step to implementation. To achieve a realistic test bench, different parameters have been considered for each diode, and all the measurements have been contaminated with noise. The results obtained show that the proposed method could be a feasible alternative for on-site calibration of six-port reflectometers.

2. Experimental set-up

The proposed identification scheme is based in the fact that the reflection coefficient S_{11} changes with the distance of the sample from the magnetron. This fact, reported in Ref. [15], allows obtaining the examples to train the network by using only one kind of material sample, which is simply placed in several different positions along the cavity. For each position of the sample, low-intensity irradiation is carried out. The measurements $\{v_3, v_4, v_5, v_6\}$ obtained from the six-port diodes and the corresponding $|S_{11}|$ coefficient constitute the input and output sides of one training example for the neural network. This method allows the use of only one sample of any material, instead of requiring several loads as in Ref. [10], thus notably simplifying the calibration process.

In order to accurately reproduce real conditions, the four diodes have been considered as having different behavior. This is simulated by using different constants in the equations of the diodes, as shown in Table 1. As the diodes are used in over a large power range, the following

Table 1
Equation of the diode and values of the constants considered for simulation

	A (V)	B (m/V)	C (m/V) ²
Diode #1	0.1153	0.4306	0.0593
Diode #2	0.0877	0.3185	0.0667
Diode #3	0.1450	0.3753	0.0479
Diode #4	0.0972	0.4364	0.0607
Equation of the diode	$v = 10A \log(1 + BE + CE^2)$		

In the equation, E corresponds to the electric field normalized by 5000 V/m.

equation has been considered to give their output voltage [12]:

$$v = 10 A \log(1 + BE + CE^2), \quad (2)$$

where E is the modulus of the electrical field detected by the diode and A , B and C are constants, which may vary from one diode to the other.

To test the method, a bidimensional cavity has been considered. This cavity, depicted in Fig. 3, is a 0.6×0.6 square in which a standard 0.12×0.08 WR-340 wave guide is placed. Inside the cavity, a 0.18×0.16 sample, with dielectric constant ϵ' and loss factor ϵ'' is placed, at a distance x from the opposite wall from the magnetron. All the measurements are given in meters.

The sample is then irradiated. To this purpose, the fundamental TE₁₀ mode was excited in the wave guide at 2.45 GHz and the module of the complex electric field has been calculated along the X-axis for each simulation.

The electromagnetic problem has been solved in the frequency domain with the aid of the vector wave Eq. (3):

$$\nabla^2 \vec{E} + \omega^2 \mu \epsilon \vec{E} = 0, \quad (3)$$

\vec{E} being the vector electric field in the multimode cavity, ω the angular frequency, μ the permeability and ϵ the permittivity of the medium. In this study, we consider non-magnetic materials characterized by its complex relative permittivity:

$$\epsilon = \epsilon' - j\epsilon'', \quad (4)$$

where ϵ' is the dielectric constant and ϵ'' the loss factor.

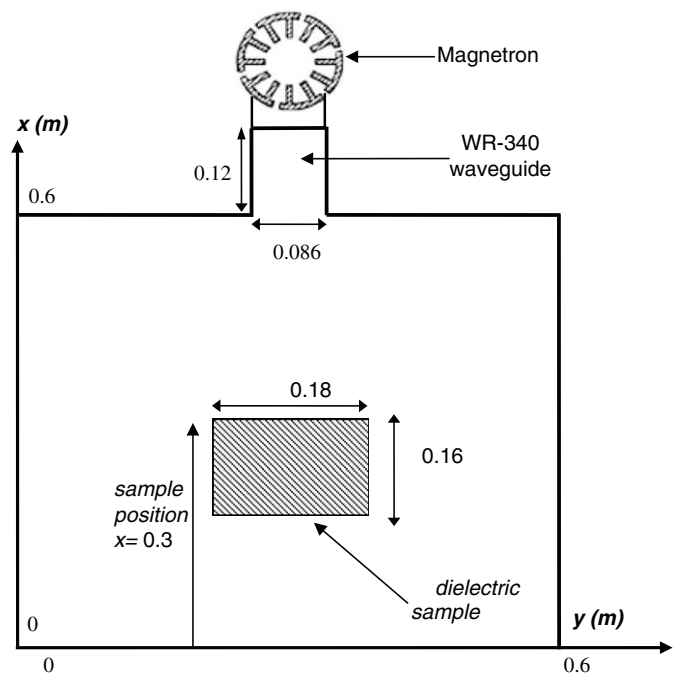


Fig. 3. Schematic representation of the microwave cavity considered in the experiments. All measures are in meters.

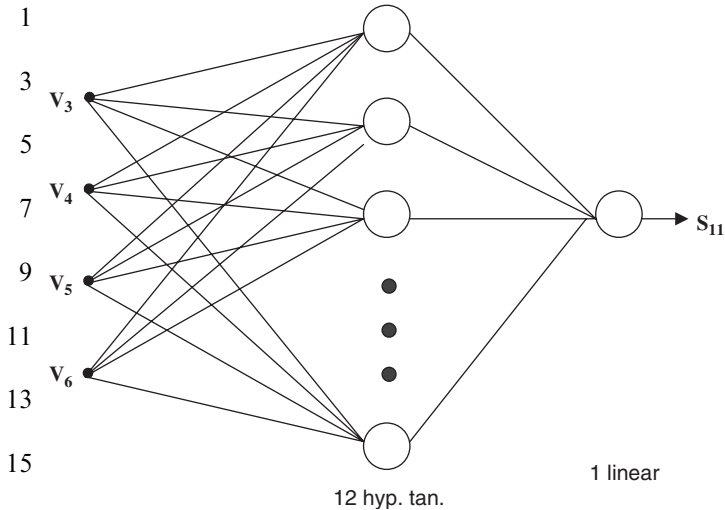


Fig. 4. Neural network scheme used in the experiments.

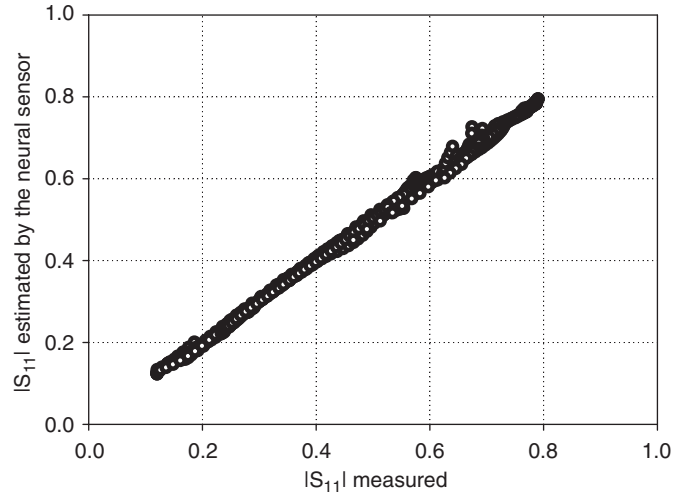


Fig. 5. Measured $|S_{11}|$ vs. $|S_{11}|$ estimated by the neural sensor. A perfect match should be represented by a straight line with a slope of 1.

The FEM has been used to solve this equation for each electric field component, by using the variational formulation as indicated in Ref. [22]. Matlab 6.0TM PDE Toolbox has been used to mesh the two-dimensional (2D) domain and to obtain the reflection coefficient for this partially filled multimode cavity. The Partial Differential Equation (PDE) Toolbox provides a MatlabTM integrated environment for the study and solution of PDEs in 2D domains and time. The PDE Toolbox supplies several tools so that the user can define a PDE problem (definition of 2D regions, boundary conditions and PDE coefficients), numerically discretize and solve the PDE equations, produce an approximation to the solution and, finally, visualize the results. Validation of this simulation tool has been previously carried out in Ref. [11].

The neural network structure has been selected to be a feedforward backpropagation-type net with two layers (Fig. 4). The first one, composed of 12 hyperbolic tangents, receives four inputs from the output voltages of the diodes on the six-port. The output layer is a linear neuron that combines the outputs of the previous layer to give the reflection coefficient.

As mentioned above, the training examples have been extracted by irradiating a material sample at different distances from the magnetron. For each position, both the measures obtained from the diodes and the reflection coefficient $|S_{11}|$ are recorded. To further reproduce the real scenario, the output of the diodes has been contaminated with white noise, whose amplitude was of a 5% of the maximum sensor range. Following this procedure, 881 samples have been extracted displacing the material at evenly spaced steps from the bottom of the cavity to the closest position to the magnetron. From these samples, 80 have been used as training examples, the rest being the validation data.

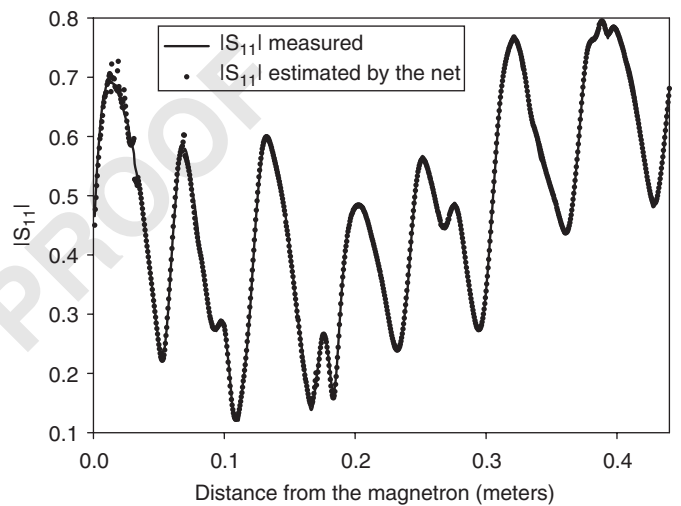


Fig. 6. Comparison between the $|S_{11}|$ values estimated by the neural sensor and the actual ones. In solid line: measured (real) values for $|S_{11}|$. In dotted line: $|S_{11}|$ estimated by the net.

3. Results

For training, 100 learning epochs of the second-order Levenberg–Mardquardt algorithm [5] have been applied. The obtained results can be observed in Figs. 5 and 6. In Fig. 5, the measured values for $|S_{11}|$ are represented against the corresponding estimations from the neural sensor. It can be seen that the relationship is almost linear. The slight deviations from linearity can be attributed to the noise in the diodes.

The accuracy achieved by the software sensor can be observed in Fig. 5. In this figure, both the real and estimated values of $|S_{11}|$ are represented against the distance from the magnetron of the sample being irradiated. It can be seen that the estimations from the neural net fit almost perfectly the measured values.

4. Conclusions

In this paper, a methodology for in situ calibration of six-port reflectometers is presented. The proposed methodology uses a neural network acting like a software sensor that infers the values of the $|S_{11}|$ reflection coefficient directly from the outputs of the diodes of the six-port. The samples employed to train the network are extracted by placing a sample of material in the microwave cavity at different distances from the magnetron, thus allowing in situ calibration, as neither especial loads nor phase shifters are needed. The results obtained in the simulation test bench corroborate the viability of the proposed method, making promising its implementation in real devices.

References

- [1] G. Colef, P.R. Karmel, M. Ettenberg, New in-situ calibration of diode detectors used in six-port network analyzers, *IEEE Trans. Instrum. Meas.* 39 (1) (1990) 201–204.
- [2] G.F. Engen, The six-port reflectometer: an alternative network analyzer, *Microwave Sympos. Dig., MTT-S Int.* 77 (1) (1977) 44–46.
- [3] G.F. Engen, Calibrating the six-port reflectometer by means of sliding terminations, *IEEE Trans. Microwave Theory Tech.* 26 (12) (1978) 951–957.
- [4] G. Engen, A least squares solution for use in the six-port measurement technique, *IEEE Trans. Microwave Theory Tech.* 28 (12) (1980) 1473–1477.
- [5] M.T. Hagan, M. Menhaj, Training feedforward networks with the Marquardt algorithm, *IEEE Trans. Neural Network.* 5 (6) (1994) 989–993.
- [6] J. Hesselbarth, F. Wiedmann, B. Huyart, Two new six-port reflectometers covering very large bandwidths, *IEEE Trans. Microwave Theory Tech.* 46 (4) (1997) 966–969.
- [7] C.A. Hoer, Performance of a dual six-port network analyzer, *IEEE Trans. Microwave Theory Tech.* 27 (12) (1979) 993–998.
- [8] S.R. Judah, W. Holmes, A novel sixport calibration incorporating diode detector non-linearity, *IEEE Instrum. Meas. Technol. Conf.* 1 (1998) 592–595.
- [9] J. Juroshek, C.A. Hoer, A high-power automatic network analyzer for measuring the RF power absorbed by biological samples in a TEM cell, *IEEE Trans. Microwave Theory Tech.* 32 (8) (1984) 818–824.
- [10] Y. Liu, Calibrating an industrial microwave six-port instrument using artificial neural network technique, *IEEE Trans. Instrum. Meas.* 45 (2) (1996) 651–656.
- [11] J. Monzó-Cabrera, A. Díaz-Morcillo, J.L. Pedreño-Molina, D. Sánchez-Hernández, A new method for load matching in multimode-microwave heating applicators based on the use of dielectric-layer superposition, *Microwave Opt. Technol. Lett.* 40 (4) (2004) 318–322.
- [12] J. Moreau, A. El Idrissi, C. Tibaudou, Permittivity measurements of materials during heating by microwaves, *Meas. Sci. Technol.* 5 (1994) 996–1001.
- [13] J.L. Pedreño-Molina, J. Monzó-Cabrera, D. Sánchez-Hernández, A new predictive neural architecture for solving temperature inverse problems in microwave-assisted drying processes, *Neurocomputing* 64 (2004) 521–528.
- [14] F. Rangel de Sousa, B. Huyart, R.N. de Lima, A new method for automatic calibration of 5-port reflectometers, *J. Microwaves Optoelectron.* 3 (5) (2004) 135–144.
- [15] M.E. Requena-Pérez, J.L. Pedreño-Molina, J. Monzó-Cabrera, A. Díaz-Morcillo, Multimode cavity efficiency optimization by optimum load location: experimental approach, *IEEE Trans. Microwave Theory Tech.* 53 (6) (2005) 2838–2845.
- [16] G. Roussv, J.A. Pearce, Foundations and industrial applications of microwave and radio frequency fields: physical and chemical processes, Wiley, New York, 1995.
- [17] T. Urbanec, J. Svačina, Software support for six-port measurement system, *Meas. Sci. Rev.* 4 (2004) 22–26 (Section 3).
- [18] F. Wiedmann, B. Huyart, E. Bergeault, L. Jallet, New structure for a six-port reflectometer in monolithic microwave integrated-circuit technology, *IEEE Trans. Microwave Theory Tech.* 46 (2) (1997) 527–530.
- [19] F. Wiedmann, B. Huyart, E. Bergeault, L. Jallet, A new robust method for six-port reflectometer calibration, *IEEE Trans. Microwave Theory Tech.* 48 (5) (1999) 927–931.
- [20] T. Yakabe, M. Kinoshita, H. Yabe, Complete calibration of a six-port reflectometer with one sliding load and one short, *IEEE Trans. Microwave Theory Tech.* 42 (11) (1994) 2035–2039.
- [21] T. Yakabe, F.M. Ghannouchi, E.E. Eid, K. Fujii, H. Yabe, Six-port self-calibration based on active loads synthesis, *IEEE Trans. Microwave Theory Tech.* 50 (4) (2002) 1237–1239.
- [22] <http://www.mathworks.com>.



Juan L. Pedreño-Molina, is Assistant Professor of Telecommunication Engineering at the Technical University of Cartagena (UPCT), Spain. He received his B.Sc. in 1984 from the Technical University of Madrid, Spain (UPM) and the Ph.D. in Neurotechnology, Control and Robotics in 2000. Since 1999 he has belonged to the Department of Information Technologies and Communications at UPCT. His research interests are in Signal Processing applied to the Control of non-linear systems, Tactile and Vision Sensors for accurate tasks with processing based on Neural Networks, and drying processes modeling.



Juan Monzó-Cabrera was born in Elda (Alicante), Spain, on January 1973. He received the Dipl. Ing. and Ph.D. degrees in telecommunications engineering from the Universidad Politécnica de Valencia, Valencia, Spain, in 1998 and 2002, respectively. From 1999 to 2000 he was a Research Assistant with the Microwave Heating Group (GCM). In 2000, he joined the Departamento de Tecnologías de la Información y las Comunicaciones, Universidad Politécnica de Cartagena, Cartagena, Spain, as an Associate Lecturer. Nowadays, he is an Associate Lecturer with the Departamento de Tecnologías de la Información y las Comunicaciones. His current research areas cover microwave-assisted heating and drying processes, microwave applicator design and optimization and numerical techniques in electromagnetics.



Miguel Pinzolas-Prado, M.Sc., Ph.D, is Senior Lecturer of System Engineering and Automation at the Technical University of Cartagena since 1999. He earned his M.Sc. degree in Physics from the University of Saragossa (1992) and his Ph.D. in Industrial Engineering from the Public University of Navarre (1997). He has been Assistant Lecturer at the Public University of Navarre and Visiting Researcher at the University of Reading. His main researching interests are related with Neural Network Learning and Applications and with Computer Vision.

1
3
5
7
9
11
13
15
17
19
21
23
25
27
29
31
33
35
37
39
41
43
45
47
49
51
53
55
57

59
61
63
65
67
69
71
73
75
77
79
81
83
85
87
89
91
93
95
97
99
101
103
105
107
109
111
113